NANO 703-Notes

Chapter 30 & 31: Image simulation and processing

Influence of C_s

Spherical aberration breaks the symmetry that would otherwise exist between overfocus and underfocus. One result is that the fringes in the FT of the CTF are generally farther apart for a given underfocus $\Delta f < 0$ than for a corresponding overfocus $\Delta f > 0$ of the same magnitude. If we don't use an OA and ignore any damping , the CTF is

$$T(u, \Delta f) = -2\sin[\chi(u, \Delta f)]$$

where

$$\chi(u, \Delta f) = \pi \cdot \left(\Delta f \cdot \lambda \cdot u^2 + \frac{1}{2}C_s \cdot \lambda^3 \cdot u^4 \right)$$

The fringes create zeros in the FT of an amorphous sample, which ideally has a continuum of spatial frequencies.

Finding C_s, Δf

Apparently, we will have extrema and zeros in the FT of the CTF given by:

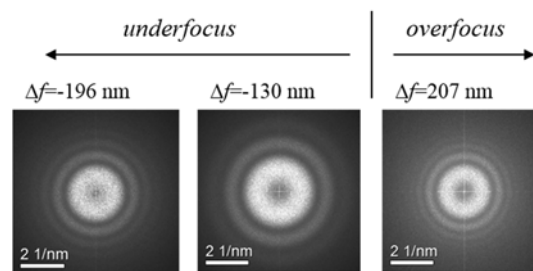$$\sin\chi(u) = \pm 1 \Rightarrow \chi(u) = \left(n + \frac{1}{2}\right) \cdot \pi$$

$$\sin\chi(u) = 0 \Rightarrow \chi(u) = n\pi$$

The zeros will occur when

$$n = \Delta f \cdot \lambda \cdot u^2 + \frac{1}{2}C_s \cdot \lambda^3 \cdot u^4$$

Analysis

One can experimentally determine C_s by analyzing FFTs acquired at different amounts of defocus.

We can measure the radii of the intensity minima in the FFT and plot their locations s as *n* vs. u^2, which can be fit to a quadratic function. The trend is clearest if we assign negative values of *n* to the zeros for underfocus. It is the slight curvature in the curves that allows us to find C_s .
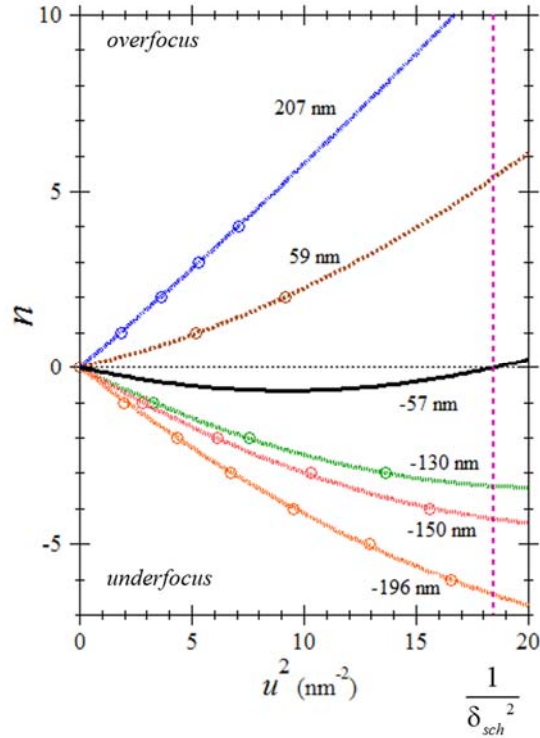
We find $C_s = 0.99$ mm. We can then proceed to find

$$\Delta f_{sch} = -\left(\frac{4}{3}C_s\lambda\right)^{1/2} = -57 \text{ nm}$$

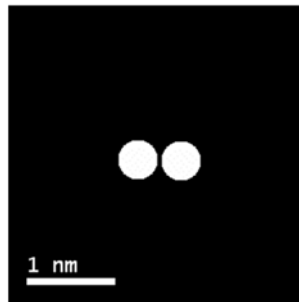and point resolution

$$\delta_{sch} = 0.66\left(C_s\lambda^3\right)^{1/4} = 0.23 \text{ nm}$$
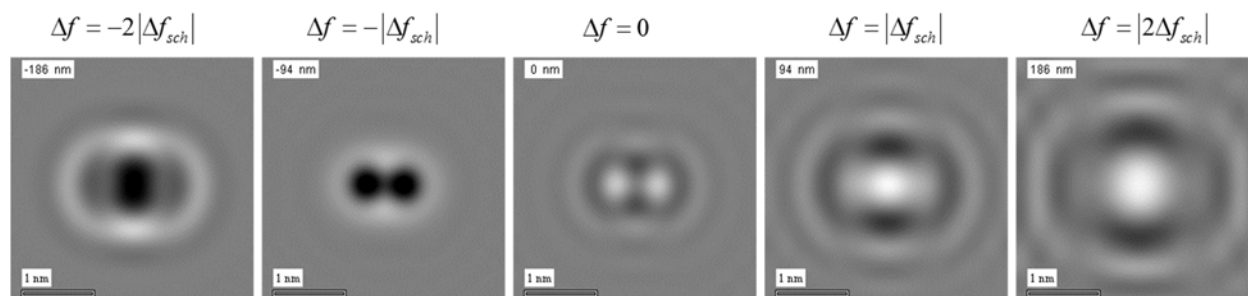
Example: phase contrast
As an simple simulation of phase contrast, we assume two closely spaced, circular phase objects separated by a distance slightly greater then δ_{sch}.

$$V(x,y)$$

Simulated images at different values of focus are shown below. We have assumed $E = 125$ KeV and $C_s = 2.0$ mm, which gives $\Delta f_{sch} = -93.7$ nm and $\delta_{sch} = 0.34$ nm.

$$\Delta f = -2\left|\Delta f_{sch}\right| \qquad \Delta f = -\left|\Delta f_{sch}\right| \qquad \Delta f = 0 \qquad \Delta f = \left|\Delta f_{sch}\right| \qquad \Delta f = \left|2\Delta f_{sch}\right|$$

While not entirely realistic, the point seems clear that the best, positive phase contrast is produced at a slight underfocus near Δf_{sch}.
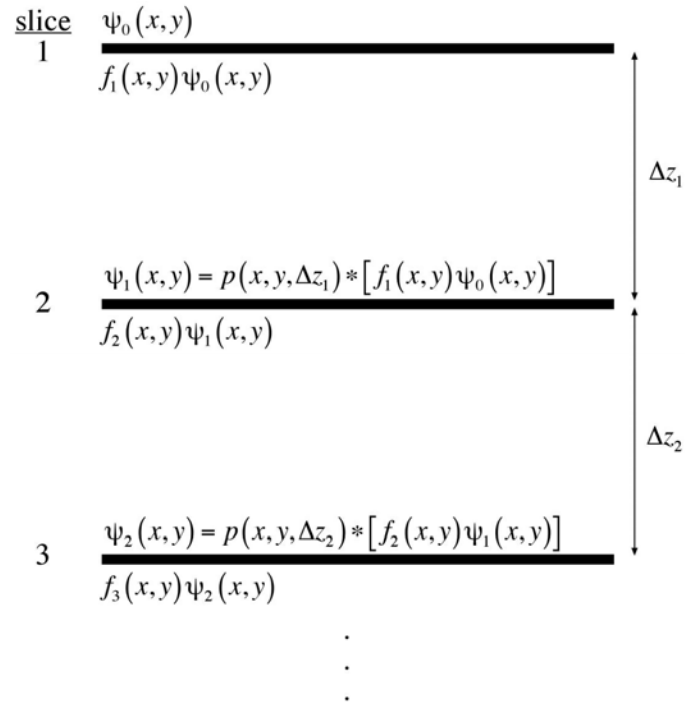
Multislice method

Multislice is another useful means to simulate images from thin specimens. A specimen is considered to contain many thin slices, perpendicular to the incident beam. It each slice is thin enough, it can be considered a weak-phase object. We can then consider the slice to be an infinitesimally thin plane represented by the projected potential. If we assume the plane lies at the top of the slice, then the rest of the slice is just vacuum. So after transmitting the incident beam through the plane, it must be propagated through the remaining thickness of the slice. This is a little more complicated than it may seem at first.
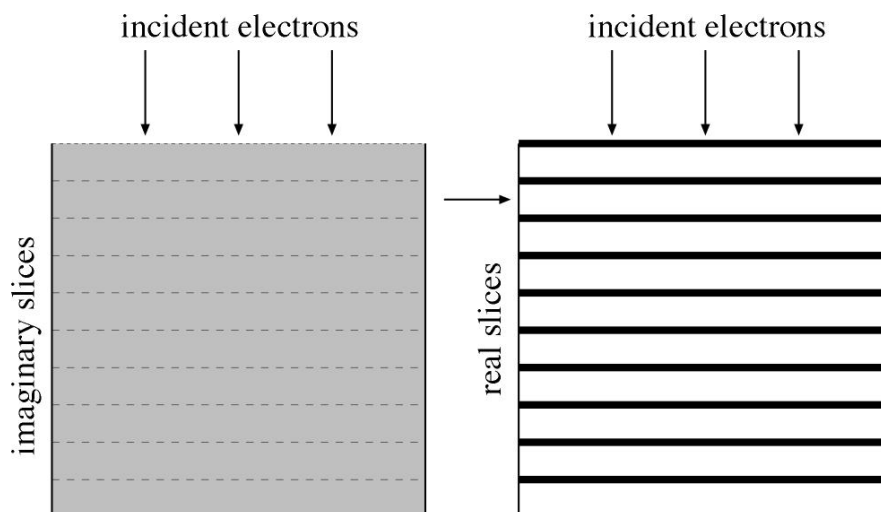

Multislice propagation

The algorithm is depicted below,. It proceed from top to bottom. First, the incident wave $\psi_0(x, y)$ is multiplied by the specimen function $f_1(x, y)$ for the first slice. Then, the product is propagated through the vacuum that comprises the slice thickness Δz_1, using the propagator $p(x, y, \Delta z_1)$, which we will derive shortly, showing that the propagation is expressed by a convolution. This gives us the incident wave $\psi_1(x, y)$ for the subsequent slice. This process is repeatedly computationally through the entire foil thickness.

$$\underset{1}{\underline{\text{slice}}} \quad \psi_0(x,y)$$

$$f_1(x,y)\psi_0(x,y)$$

$$\Delta z_1$$

$$2 \quad \psi_1(x,y) = p(x,y,\Delta z_1) * [f_1(x,y)\psi_0(x,y)]$$

$$f_2(x,y)\psi_1(x,y)$$

$$\Delta z_2$$

$$3 \quad \psi_2(x,y) = p(x,y,\Delta z_2) * [f_2(x,y)\psi_1(x,y)]$$

$$f_3(x,y)\psi_2(x,y)$$

.
.
.

If every slice has the same projected potential, the specimen function only needs to be computed once, but this is not a strict requirement. But one can imagine applying the method on a zone axis, where every slice represents a crystallographic lattice plane of the specimen.

Propagator
We used Huygens' principle to explain why diffraction occurs from a narrow slit. After an incident wave is transmitted through a thin plane (object) we should consider contributions to a point on a subsequent plane (image) from the spherical wavelets emitted at every point on the exit surface of the object. These wavelets reaching our image point have different path lengths and make different angles q w.r.t the incident wave direction.
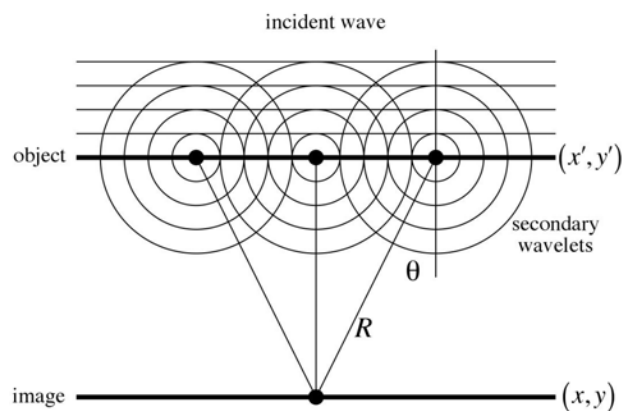
Deriving the propagator
The formalism here is based on the Fresnel-Kirchhoff integral.:

$$\psi(x,y,z+\Delta z) = -ik \int\limits_{source} \psi(x',y',z) \cdot \frac{e^{2\pi ikR}}{R} \cdot \left(\frac{1+\cos\theta}{2}\right) dx'dy'$$

NANO 703-Notes

In TEM, we can fortunately make the small-angle approximation when evaluating the "obliquity factor":

$$\frac{1+\cos\theta}{2} \approx 1$$

The radius is given by

$$R = \sqrt{(x-x')^2 + (y-y')^2 + (\Delta z)^2}$$

Because the angles are small, we assume lateral separations are much less then the slice thickness. So the phase factor becomes

$$e^{2\pi ikR} \approx e^{2\pi ik \cdot \Delta z} \cdot e^{\pi ik \cdot \Delta z \cdot \left[\left(\frac{x-x'}{\Delta z} \right)^2 + \left(\frac{y-y'}{\Delta z} \right)^2 \right]}$$

The denominator is

$$\frac{1}{R} \approx \frac{1}{\Delta z} \cdot \left[1 - \frac{1}{2}\left(\frac{x-x'}{\Delta z} \right)^2 - \frac{1}{2}\left(\frac{y-y'}{\Delta z} \right)^2 \right]$$

Combining these, keep only lowest-order corrections, we have

$$\frac{e^{2\pi ikR}}{R} \approx \frac{e^{2\pi ik \cdot \Delta z} \cdot e^{\frac{\pi ik}{\Delta z}\left[(x-x')^2 + (y-y')^2 \right]}}{\Delta z}$$

The wave at the bottom of the slice is then

$$\psi(x,y,z+\Delta z) \approx -ik\frac{e^{2\pi ik \cdot \Delta z}}{\Delta z} \int\limits_{x',y'} \psi(x',y',z) \cdot e^{\frac{\pi ik}{\Delta z}\left[(x-x')^2 + (y-y')^2 \right]} dx'dy'$$

Notice that this has the form of a 2-D convolution of our transmitted wave with…something.

The propagator function
We can write this convolution as

$$\psi(x,y,z+\Delta z) = e^{2\pi ik \cdot \Delta z} \int\limits_{x',y'} \psi(x',y',z) \cdot p(x-x', y-y') dx'dy'$$

where we have defined the propagator

$$p(x,y) = \frac{-ik}{\Delta z} \cdot e^{\frac{\pi ik}{\Delta z}(x^2+y^2)}$$

Also, there is no good reason to keep the phase factor $\exp(2\pi ik \cdot \Delta z)$, since the overall phase is arbitrary. So

$$\psi(x,y,z+\Delta z) = \psi(x,y,z) * p(x,y,\Delta z)$$

Multislice algorithm
Here is what we have so far. The wave function below slice $n+1$ is given by

NANO 703-Notes

$$\psi_{n+1}(x,y) = p(x,y,\Delta z_{n+1}) * [f_{n+1}(x,y) \cdot \psi_n(x,y)]$$

We need to transmit the wave through the projected potential for a slice, propagate through the vacuum that comprises the rest of the slice, then repeat. Symbolically

$$\psi_1 = p(\Delta z_1) * [f_1 \cdot \psi_0]$$
$$\psi_2 = p(\Delta z_2) * [f_2 \cdot \psi_1] = p(\Delta z_2) * [f_2 \cdot [p(\Delta z_1) * [f_1 \cdot \psi_0]]]$$
$$\vdots$$

Multislice in reciprocal space

Convolutions are often easier to perform by combining them with Fourier transforms. The convolution theorem tells us

$$\Im\{\psi_{n+1}(x,y)\} = \Im\{p(x,y,\Delta z)\} \cdot \Im\{f_{n+1}(x,y) \cdot \psi_n(x,y)\}$$

We need to know the 2-D FT of the propagator. A little thought shows that

$$\Im\{p(x,y,\Delta z)\} = p(u_x, u_y, \Delta z) = e^{-\pi i \left(u_x^2 + u_y^2\right)\Delta z / k}$$

Now

$$\psi_{n+1}(x,y) = \Im^{-1}\left\{ e^{-\pi i \left(u_x^2 + u_y^2\right)\Delta z_n / k} \cdot \Im\{f_{n+1}(x,y) \cdot \psi_n(x,y)\}\right\}$$

We can multiply the incident wave by the specimen function, take the FT, multiply that by the FT of the propagator, then perform an inverse FT to find the incident wave on the next slice.

Note that, to use FFTs, we will want to ensure periodic boundary conditions for our projected potential. Otherwise, artifacts show up from edge effects. Also note that even single atomic layers or some materials may not be pure phase objects. For example, it is argued by some that single Au atoms are not pure phase objects. So we would need to slice up atomic planes to perform accurate simulations of these materials using multislice.

Simulations: spherical particle, multislice

Notice that the Bloch-wave method assumed an infinite crystal. So it is not practical to use Bloch waves to simulate data from less ideal objects, like nanoparticles. Below are shown some multislice simulations using a reasonably realistic model of a spherical, crystalline nanoparticle . One set of lattice planes is included to show their appearance in the images. Cross sections of this object at very small increments were used to compute the projected potentials for each slice. It was assumed that $E = 200 \text{ KeV}$ and $C_s = 2.0 \text{ mm}$. A simple quadratic damping with $\alpha_{damp} = 2.0 \text{ nm}^{-1}$ was included to make the simulations a bit more realistic.
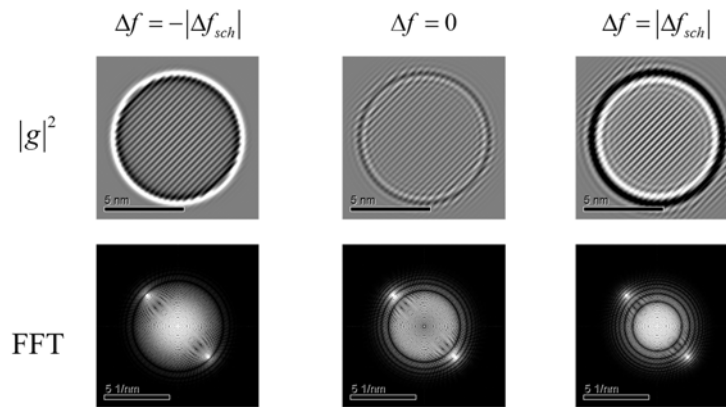
The image at the Scherzer defocus (underfocus) shows the best positive phase contrast with the fewest artifacts. The in-focus image has fairly low contrast, while the overfocus image has negative phase contrast. The overfocus also shows delocalization of the lattice fringes. This is because perfect spatial coherence was assumed in the calculation.